

## FULL-WAVE NONLINEAR ANALYSIS OF MICROWAVE SUPERCONDUCTOR DEVICES : APPLICATION TO FILTERS

Mohamed A. Megahed and Samir M. El-Ghazaly

Department of Electrical Engineering  
 Telecommunications Research Center  
 Arizona State University  
 Tempe, AZ 85287-5706

### ABSTRACT

A full-wave three-dimensional nonlinear HTS finite-difference time-domain electromagnetic simulator is developed. The HTS nonlinear model, based on the Ginzburg-Landau theory, is blended with Maxwell's equations. The analysis is performed in time domain, which is necessary for modeling the nonlinear aspects of microwave superconductor devices. The fields in the superconducting device are calculated. Interesting aspects of the nonlinearity in a superconducting material are observed. Applications to microstrip line and filters are presented.

### INTRODUCTION

High temperature superconductor transmission line resonators in narrow band filters have peak current densities, which result from the high standing-wave ratios on the resonator lines. This high current value may not exceed the high temperature superconductor (HTS) critical current densities of high-quality YBCO films, but they are high enough to drive the HTS into nonlinear behavior. This nonlinearity associated with HTS can not be ignored for the microwave and millimeter-wave superconducting devices in general. Better understanding for the dependence of the penetration depth inside the superconducting material as well as the normal conductivity on the microwave magnetic field requires a rigorous nonlinear model. This model must only be implemented in the time domain. If such a model is implemented in frequency domain, unreliable results may be obtained. In this paper, non linear full-wave model, based on the Ginzburg-Landau (GL) theory, is developed using the finite-difference time-domain (FDTD) technique. First, this time-domain nonlinear approach is successfully used to predict the effects of the nonlinearity

on the performance of the HTS transmission lines. Then, it is extended to analyze and study the nonlinearity effects on HTS microwave filters. This approach is not only useful to predict the nonlinearity effects on microwave devices performance but also can be utilized in the characterization of the HTS materials.

### NONLINEAR SUPERCONDUCTING MODEL

Ginzburg and Landau (GL) equations, which are an accepted phenomenological formulation for describing the superconducting behavior used in microwave and millimeter-wave devices operating in the low gigahertz region, are used to describe the macroscopic characteristics of the HTS material. These equations allow for spatial variations in the superconducting electron density in the presence of a magnetic field. The normalized GL equations for calculating the superfluid z-component can be simplified to the following form:

$$\frac{1}{\kappa^2} \nabla_t^2 |\psi| = |\psi| \left( |\psi|^2 - 1 + \frac{A_z^2}{2} \right) \quad (1)$$

$$\nabla_t^2 A_z = |\psi|^2 A_z \quad (2)$$

where  $t$  stands for the transverse x-y direction. The required boundary conditions are

$$\hat{n} \times (\nabla_t \times \hat{z} A_z) = \mu_0 \bar{H}_t \quad (3)$$

$$\hat{n} \cdot \nabla_t |\psi| = 0. \quad (4)$$

The order parameter  $\psi$  is taken as a complex function and is interpreted as analogous to a wave function for superconductor fluid [1]. The first nonlinear GL equation, which resolves the order parameter, is solved using a Newton-SSOR iteration scheme. The second GL equation, which corresponds to the superconducting current, is manipulated using a linearized scheme. Details of this approach can be found elsewhere [2]. The results calculated for the one-dimensional case show excellent agreement with published data [3]. The two-dimensional simulation results are presented in [2] for both the linear

TH  
 3C

and nonlinear distributions of the superconducting current inside an HTS strip. It is clear that the HTS material can be driven into nonlinearity and even loses its superconducting characteristics near the edge of the strip. These results assure that the GL formulation can be successfully used to describe the nonlinearity inside the HTS material. The obtained superconducting current, and order parameter are used as inputs to the electromagnetic model. They are field and space dependent. Alternatively, the macroscopic parameters of the HTS, the normal conductivity and the penetration depth, can be directly modified according to the field and space dependent order parameter, using the conservation of charge law. In fact, the order parameter corresponds to the number of superconducting electrons in the mixed state HTS material. Then, the updated macroscopic parameter can be inserted directly into a simpler formulation as London's equation resulting in a simpler nonlinear macroscopic representation for the HTS materials, which can be used for computer-aided-design and analysis of HTS microwave devices.

## TIME-DOMAIN ELECTROMAGNETIC MODEL

A full wave analysis is performed using the three-dimensional finite-difference time-domain method (FDTD). The FDTD is a powerful tool to solve for the fields inside the superconducting microwave structures, where nonlinearity is expected. Moreover, the entire frequency spectrum of interest can be analyzed by using a broad-band pulse. Also, nonisotropic substrates or HTS materials can be easily represented. One must note that the time-domain approach is the most accurate method applicable to study nonlinear phenomena. A graded non uniform mesh generator is used along the cross section of the microstrip, which allows us to represent it by an adequate number of mesh points [4]. A time domain history, governed by the amplitude of the magnetic field underneath the strip, is used to excite the microwave transmission line. The computational domain is enclosed by using the perfectly matched layers absorbing boundary conditions.

## NONLINEAR 3-D FULL-WAVE HTS MODEL

The nonlinear superconducting model is incorporated into the 3-D full-wave electromagnetic simulator. The superconducting current is directly included into Maxwell's equations. The conductivity of normal electrons depends on the change in the order parameter, and is expressed as follows:

$$\sigma_n(H(\bar{r}), T) = \sigma_n(H_c/T_c) \left[ 1 - \left\{ \begin{array}{l} \left( \frac{\psi(H(\bar{r}), T)}{\psi(0, T)} \right)^\alpha \\ * \left( 1 - \left( \frac{T}{T_c} \right)^\beta \right) \end{array} \right\} \right] \quad (5)$$

where  $\sigma_n(H_c/T_c)$  is the maximum normal conductivity measured either at  $T = T_c$  or  $H = H_c$  and  $H_c$  is the critical magnetic field for the superconductor calculated at  $T = 0$ . The parameters  $\alpha$  and  $\beta$  may be obtained from experimental studies. In our analysis, we chose  $\alpha = 2$  and  $\beta = 4$  following GL model for the field dependence and Gorter-Casimir for the temperature approximations. The corresponding spatial, field and temperature dependent magnetic field penetration depth  $\lambda_s$  for the superconductor is obtained from the following expressions

$$\lambda_s(H(\bar{r}), T) = \frac{\lambda_s(0, 0)}{\sqrt{\left( \frac{\psi(H(\bar{r}), T)}{\psi(0, T)} \right)^\alpha * \left( 1 - \left( \frac{T}{T_c} \right)^\beta \right)}} \quad (6)$$

where  $\lambda_s(0, 0)$  is the low field penetration depth measured at  $T = 0$  and  $H = 0$  and  $T_c$  is the critical temperature for the superconductor calculated at  $H = 0$ . Eq. 5 and 6 are one of the main results of this paper. They are updated with the propagation of the wave along the microstrip line. Thus, the macroscopic parameters of the superconducting material are fully included in the structure. An alternative scheme is to develop a phenomenological equation, based on the GL formulation, for the order parameter. It is obvious that the normalized order parameter will be a function of the applied magnetic field and the position from the surface of the HTS film. Using this order parameter, the nonlinear normal conductivity as well the superconducting penetration depth can be calculated. Then, the updated nonlinear HTS macroscopic parameters are incorporated into Maxwell's using the two fluid model. A discussion of this model is beyond the scope of this paper.

## RESULTS AND DISCUSSION

The nonlinearity effects is first examined on the microstrip line shown in Fig. 1. The microstrip line is used later in the analysis of the microstrip line bandpass HTS filter presented in Fig. 2. The results are obtained for  $\text{YBa}_2\text{Cu}_3\text{O}_{7-x}$  superconducting microstrip line, with critical temperature of 90K, critical magnetic flux density  $\mu_0 H_c$  of 0.17, and GL parameter of 44.8 at 77K. The superconducting microstrip line has a strip width of 7.5  $\mu\text{m}$ , and a thickness of 1  $\mu\text{m}$ . The substrate thickness is 10

$\mu\text{m}$ , with  $\epsilon_r = 13$ . The transmission line characteristics are simply chosen to demonstrate the nonlinear wave propagation along the line. The maximum rf power,  $P_{\text{crf}}$ , where the HTS microstrip looses completely its superconductivity, is predicted using GL solution. Its value equals to  $920 \text{ W/cm}^2$  [5]. The fractional change in the effective dielectric constant at different power levels obtained from GL model with respect to the one calculated using London's theory is drawn in Fig. 3. The change in the effective dielectric constant increases with the increase in the power level up to  $0.7 P_{\text{crf}}$ . It is approximately constant for higher power levels, where almost complete field penetration occurs. The fractional change in the attenuation constant obtained from GL model with respect to the value predicted by London model at 10 GHz is depicted in Fig. 4. It is clear that the HTS looses its superconductivity very quickly as the applied power approaches the rf critical power,  $P_{\text{crf}}$ . Also, the nonlinearity associated with the HTS appears very early, even with the material in fairly good superconducting stage. The change in the losses is faster and more nonlinear than the change in the phase velocity. The effect of the nonlinearity on the frequency spectrum of the wave propagating along the line is analyzed in Fig. 5. The fractional change in the amplitude of the output pulse frequency components increases with the applied power. It is observed that as the power level increases, the amplitudes of the different harmonics change, which is one of the primarily characteristics of nonlinear devices. This confirms our point that the nonlinearity has to be modeled in the time domain.

A simulation for the microstrip resonator array filter using our full-wave 3-D nonlinear HTS FDTD electromagnetic simulator, which rigorously includes the finite thickness of the HTS film, is performed. The filter configuration is shown in Fig. 2. Despite of the difficulty and the complexity of the filter structure, our model was able to successfully present all the different aspects of the filter. The graded non uniform mesh generator allows us to represent the filter with adequate number of 3-D nodes, which can be handled by the available computer resources. The wave propagating along the filter is shown in Fig. 6. The program code is written in FORTRAN 90 and is executed in massively parallel machine (MASPAR) environment. Fig. 7 shows the calculated  $S_{21}$  parameter of the filter up to 25 GHz. The small bandwidth of the filter is precisely predicted by our simulation approach. The capability of our developed model to simulate the filter is proved by the second resonance peak at double the operating frequency of the filter due to its periodic design as expected. The  $S_{21}$  parameter depicted from our simulation agrees with the  $S_{21}$  obtained from the measurement and shown in Fig. 8. The calculated central frequency at 8.67 GHz as well as the bandwidth precisely matches the measured ones. Our model is capable of predicting the change in the filter response with the power level.

## CONCLUSION

A full-wave three-dimensional nonlinear HTS finite-difference time-domain electromagnetic simulator is developed. This model is flexible and can be applied to different HTS microwave and millimeter-wave devices. The variation of the macroscopic parameters of the superconducting material with the applied magnetic field and positions, as well as the wave propagation inside the superconducting material are rigorously presented. The nonlinearity associated with HTS is successfully simulated. Results obtained for five-pole HTS filter agrees well with the measured ones.

## ACKNOWLEDGMENT

The authors would like to thank Ali Fathy from David Sarnoff lab for supplying the measured data for the high Q filter. This work was supported by the National science foundation under Grant ECS-9108933.

## REFERENCES

- [1] R. D. Parks, *Superconductivity* (in two volumes). New York : Marcel Dekker, 1969.
- [2] M. A. Megahed and S. M. El-Ghazaly, "Analysis of Waveguides with Nonlinear Material : Applications to Superconductor Microstrip lines" *24<sup>th</sup> Europ. Microw. Conf. Symp. Dig.*, Sep. 1994.
- [3] Cheung-Wei Lam, D. M. Sheen, S. M. Ali, D. E. Oates, "Modeling the nonlinearity of superconducting strip transmission lines," *IEEE Trans. on App. Superconductivity*, vol. 2, no. 2, pp. 58-65, 1992.
- [4] M. A. Megahed and S. M. El-Ghazaly, "Finite Difference Approach for rigorous full-wave analysis of superconducting microwave structures" *IEEE MTT-S Int. Symp. Dig.*, June 1993, pp. 499-508.
- [5] M. A. Megahed and S. M. El-Ghazaly, "Nonlinear analysis of Microwave Superconducting Devices using Full-Wave Electromagnetic Model" submitted to *IEEE Tans. Microwave Theory Tech.*

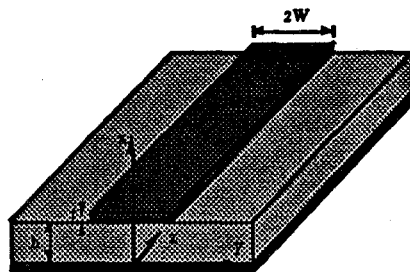


Fig. 1 HTS microstrip line geometry

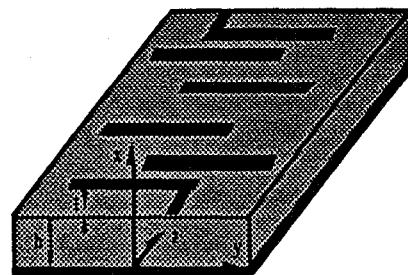


Fig.2 HTS microstrip array filter on thallium substrate

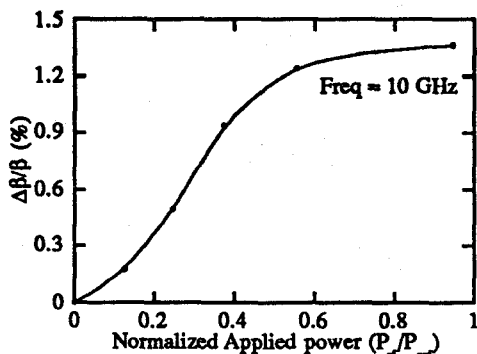


Fig.3 Fractional change in the effective dielectric constant for HTS microstrip line with applied power w.r.t the linear model

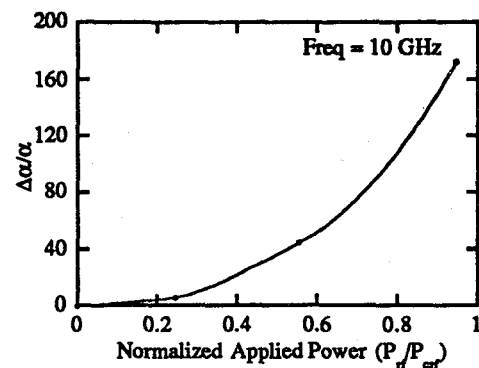


Fig.4 Fractional change in the attenuation constant for HTS microstrip line with applied power w.r.t the linear model

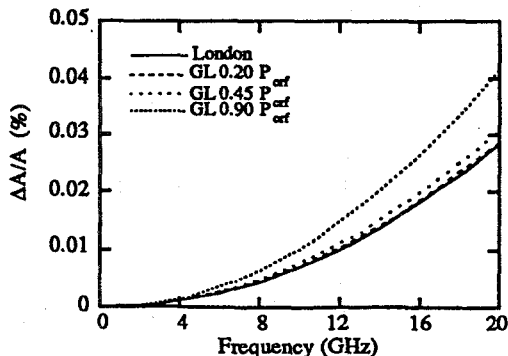


Fig.5 Fractional change in the amplitude of the frequency spectrum of the output pulse w.r.t. the dc component at different applied power levels.

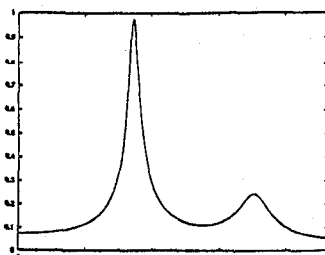


Fig.7 Calculated  $S_{21}$  for the microstrip line band pass filter

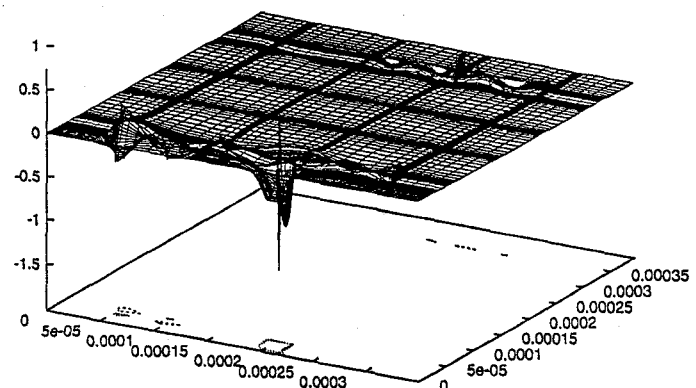


Fig.6 FDTD nonuniform mesh distribution along the simulated filter with H field component parallel to the HTS strip surface

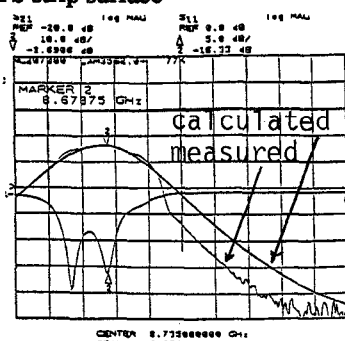


Fig.8 Calculated and measured  $S_{21}$  comparison